ACS APPLIED MATERIALS & INTERFACES

Research Article

www.acsami.org

Conductive Nanocomposites Based on Polystyrene Microspheres and Silver Nanowires by Latex Blending

Manthiriyappan Sureshkumar,[†] Hyo Yeol Na,[‡] Kyung Hyun Ahn,[§] and Seong Jae Lee*[,‡]

[†]Department of Chemistry and [‡]Department of Polymer Engineering, The University of Suwon, Hwaseong, Gyeonggi 445-743, Republic of Korea

[§]School of Chemical and Biological Engineering, Institute of Chemical Process, Seoul National University, Seoul 151-744, Republic of Korea

Supporting Information

ABSTRACT: Metallic nanowires with excellent electrical conductivity and high aspect ratio are critical in the preparation of conductive polymer nanocomposites. In this work, highly conductive polystyrene/silver nanowire (PS/AgNW) nanocomposites were prepared by latex blending, and their electrical and rheological properties were investigated. A high yield of long and thin AgNWs was synthesized with the polyol method. AgNWs were incorporated with highly monodisperse PS microspheres to produce polymer nanocomposites with a nanowire network structure providing electrical pathways. An electrically conductive network of AgNWs was obtained at an electrical percolation threshold of 0.49 vol % AgNW, and an electrical conductivity of 10^2 S/m was obtained at 1 vol %. The dynamic rheological properties evaluated at 1 vol % also confirmed that the AgNWs were physically connected to one another at this concentration.

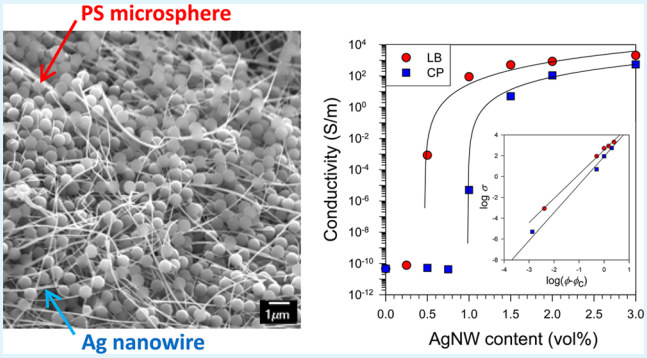

KEYWORDS: *nanocomposites, polystyrene, silver nanowires, latex blending, rheological properties, electrical conductivity*

1. INTRODUCTION

Polymer nanocomposites have attracted a great deal of research attention in recent years and have tremendous potential for a variety of high-performance composites, sensors, catalysts, and electronic and optoelectronic devices.[1] Nanocomposites usually have excellent mechanical, thermal, and electrical properties compared to conventional composites. In particular, conducting polymer nanocomposites are very fascinating materials that combine the key features of polymers, namely, lower cost, lightweight, and ease of processing, with the conductive properties of nanomaterials and thus create potentially the next generation of hybrid materials.[2] The electrical conductivity of a polymer can be improved by the inclusion of conductive fillers into an insulating polymer. One-dimensional (1D) nanofillers such as nanowires, nanorods, and nanotubes have had an important role in the development of conductive polymer nanocomposites.[3] Compared to the zero-dimensional (0D), two-dimensional (2D), and three-dimensional (3D) nanomaterials, the smaller dimension and higher aspect ratio of 1D nanomaterials effectively carry electrical carriers along one controllable path and have demonstrated that increasing the aspect ratio of nanofillers will ultimately increase the conductivity of nanocomposites.[4] In conductive polymer nanocomposites, there is a critical concentration for which the nanofillers within the polymer matrix form a random conductive network, and then, the composites change from insulative to conductive. This concentration is known as the percolation threshold, which is characterized by a sharp drop of several orders of magnitude in resistivity.[5] 1D nanofillers with a well-controlled structure will reduce nanofiller loadings in polymer nanocomposites.[6] Especially, carbon nanotubes (CNTs) and metallic nanowires with a high aspect ratio are used to build conducting polymer nanocomposites with fine electrical properties and a low electrical percolation threshold. Major applications of conductive polymer nanocomposites are electromagnetic interference (EMI) shielding materials and electrostatic discharge (ESD), for which electrical conductivities (>1 S/m for EMI and 10^{-6}–10^{-2} S/m for ESD) are typically required.[7,8] Low concentrations of conductive nanofillers homogeneously dispersed also retain the mechanical properties of the polymer matrix.[9] It is expected that distinct properties from the polymer matrix and metallic nanowires will be exhibited in the conducting polymer nanocomposites.

Although many different metallic nanowires have been investigated to produce conductive nanocomposites, AgNW-based studies have drawn huge interest from different research groups.[10,11] Random networks of AgNWs are promising candidates for conductive devices. As a result, AgNW-based

Received: October 17, 2014
Accepted: December 15, 2014
Published: December 24, 2014

DOI: 10.1021/am5071392
ACS Appl. Mater. Interfaces 2015, 7, 756–764

polymer nanocomposites have been examined for a number of applications including chemical and biological sensors, EMI shielding, thermal interface materials (TIMs), flexible optoelectronic devices such as solar cells and organic light-emitting devices (OLEDs), and actuators.[11−15] Over the past few years, many synthetic methods to prepare conductive AgNWs have been reported. In prior works, AgNWs have been synthesized by different methods such as solvothermal synthesis,[16] electrochemical deposition,[17] polyol method[18−21] and microwave-aided synthesis.[22] Highly conductive AgNWs are easily prepared by the polyol method. In this technique, ethylene glycol is used as a solvent and mild reducing agent. Mild reduction of silver nitrate in the presence of poly(vinylpyrrolidone) (PVP) in ethylene glycol is able to produce uniform AgNWs. The size and shape of the AgNWs can be tuned by adjusting the concentration of the reactants, the reaction temperature, the solvent, and PVP concentrations.

To achieve good dispersion of nanofillers and to enhance the electrical conductivity of the polymer nanocomposites, several techniques have been routinely investigated.[10] To develop efficient conductive nanocomposites has one key bottleneck issue: nanofillers may form aggregates or bundles in the polymer matrix,[23] which will damage the conductive nature of the nanocomposites. The agglomeration or dispersion of nanofillers in a polymer matrix depends on dispersion conditions, alignment of nanowires, surface treatments, processing conditions, and properties of the polymer matrix. As a result, the dispersion and incorporation of nanofillers into a polymer matrix is one of the most vital and challenging steps toward capitalizing the advantages of using nanofillers. Many alternative techniques have been introduced to produce nanocomposites with high electrical conductivity.[24,25] In recent literature, latex blending has been shown to be a prominent, simple, and convenient technique to prepare polymer nanocomposites.[26,27] To our knowledge, however, there are no reports on the preparation and properties of PS/AgNW nanocomposites by latex blending.

In this work, the advantages of using latex blending to produce conductive nanocomposites are shown. First, uniform and well-dispersed AgNWs were synthesized by means of the polyol method. Monodisperse PS microspheres were prepared by the emulsifier-free emulsion polymerization method, which were used as the polymer matrix to obtain conductive nanocomposites. Electrically conductive PS/AgNW nanocomposites were prepared with the latex-blending method. Next, field emission-scanning electron microscopy (FE-SEM), energy-dispersive X-ray spectroscopy (EDS), UV−visible (UV−vis) absorption spectrometry, X-ray diffraction (XRD), X-ray photoelectron spectroscopy (XPS), and thermogravimetric analysis (TGA) were done to characterize the prepared nanomaterials. Lastly, the electrical and rheological properties of the PS/AgNW nanocomposites as end-use properties were investigated.

2. EXPERIMENTAL SECTION

Materials. Silver nitrate ($AgNO_3$) was purchased from Kojima (Japan). Styrene monomer and ethylene glycol were purchased from Samchun Chemical (Korea). PVP (MW = 1 300 000 g/mol), copper(II) chloride ($CuCl_2$), and potassium persulfate were purchased from Aldrich. For all experiments, deionized water purified by Option-Q (Purelab, ELGA) was used. Styrene monomer was purified by vacuum distillation before use. The other solvents and reagents were used without further purification.

Synthesis of PS Microspheres. Submicron-sized monodisperse PS microspheres were synthesized in a three-neck double-jacket Pyrex reactor by emulsifier-free emulsion polymerization of styrene monomers under a nitrogen atmosphere. In a typical PS microsphere synthesis, 40 mL of styrene and 0.3676 g of potassium persulfate were added to a reactor containing 43.2 mL of ethanol and 360 mL of deionized water. Polymerization was done at 70 °C for 24 h with an agitation speed of 300 rpm.

Synthesis of AgNWs. AgNWs were synthesized with the polyol method.[20] Synthesizing AgNWs involves the formation of metal seeds by ethylene glycol reduction of $AgNO_3$, and then, AgNWs grow on the previously formed seeds. Here, ethylene glycol acts as a solvent and reducing agent. Key factors affecting the formation of AgNWs are the precursor concentration, addition rates, and molar ratio between the repeating unit of PVP and $AgNO_3$.[19] In a typical procedure, 5 mL of ethylene glycol was preheated at 150 °C for 1 h under continuous stirring at 260 rpm. Then 40 μL of a 4 mM $CuCl_2{\cdot}2H_2O$/ethylene glycol solution was added, and the solution was allowed to heat for 15 min. Subsequently, 1.5 mL of 114 mM PVP/ethylene glycol followed by 1.5 mL of 94 mM $AgNO_3$/ethylene glycol was added dropwise. Magnetic stirring was continuously done throughout the silver ion reduction and nanowire growth process. The reaction mixture was heated to 160 °C and stirred at 600 rpm. The reaction was stopped when the solution became gray and wispy after approximately 1 h. The reaction was stopped by submerging the vials into cold water. The AgNWs were thoroughly washed with acetone and deionized water to remove any unreacted reactants, nanoparticles, and/or nanorods, as seen in Figure S1 in the Supporting Information for a comparison of the AgNWs before and after purification. Purified AgNWs were stored in a refrigerator for further modification.

Preparation of PS/AgNW Nanocomposites. To achieve agglomeration-free conductive PS/AgNW nanocomposites, the latex-blending technology was used.[26,27] First, AgNWs were completely dispersed in deionized water. To incorporate AgNWs into a polymer matrix, the AgNWs were homogeneously mixed with the appropriate amount of PS latex while keeping the mixture in an ultrasonication bath at 20 W for 30 min, and then, the mixture was abruptly frozen with liquid nitrogen. The aqueous moiety in the frozen mass was removed by freeze-drying (FD-1000, EYELA). Finally, the freeze-dried PS/AgNW composite powder was compressed into 1−2 mm thick disk-type samples with a diameter of 25 mm at 180 °C for 5 min using a hot press. PS/AgNW nanocomposites were prepared by varying the AgNW content (1 and 3 vol %). Figure 1 shows a schematic of the procedure for the preparation of the PS/AgNW nanocomposites by latex blending. For comparison with the latex technology, a coagulated precipitation sample was also prepared with the following steps. To begin with, AgNWs were dispersed in a PS solution dissolved in toluene. Next, the mixture was precipitated in water as a coagulant, and then, disk-type samples were prepared by collecting the precipitates and completing the subsequent compression molding as described above.

Characterization. The morphology and size of the AgNWs, PS microspheres, PS/AgNW composite powder, and the nanocomposites were investigated with SEM (JSM 5200, JEOL) and FE-SEM (JSM 6700F, JEOL) with EDS, in which EDS is a characterization method providing information on a sample's elemental composition. The dispersion state of the AgNWs was checked by freeze-fracturing the PS/AgNW nanocomposites, and the fracture surface was analyzed with FE-SEM. Powder XRD measurements of the dried AgNWs were recorded using a diffractometer (D8 Advance, Bruker) with Cu Kα radiation. UV−vis absorption spectra were obtained on a spectrophotometer (Shimadzu UV-250). Thermal analysis of the PS/AgNW nanocomposites was determined by TGA (STA 409, Netzsch) using a temperature sweep from 25 to 600 °C with a heating rate of 20 °C/min. The nature of the AgNWs was also verified with an XPS instrument (Sigma Probe, Thermo Scientific).

The rheological properties of the PS/AgNW nanocomposites were investigated with a rotational rheometer (MCR 300, Anton Paar) in small-amplitude oscillatory shear mode using parallel plate geometry. Frequency sweeps between 0.03 and 100 s^{-1} were performed at a

DOI: 10.1021/am5071392
ACS Appl. Mater. Interfaces 2015, 7, 756−764

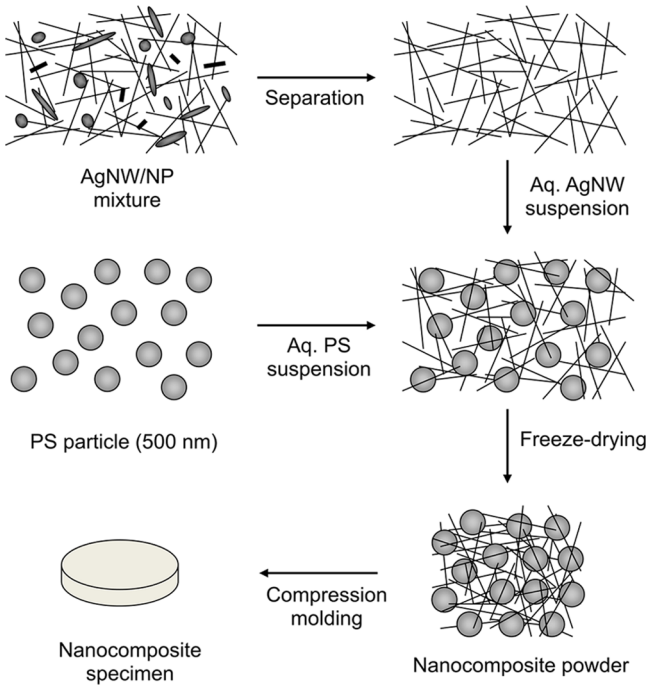

Figure 1. Schematic of the procedure for preparing PS/AgNW nanocomposites with the latex-based process.

strain amplitude of 3% throughout the measurements, after confirming that the amplitude was within the linear viscoelastic range. All measurements were conducted at a constant temperature of 210 °C. The electrical resistance of the PS/AgNW nanocomposites prepared either by latex blending or by coagulated precipitation was measured with a picoammeter (Keithley 6487) and a digital multimeter (Fluke 189). After polishing the sample to eliminate the polymer-rich layer, silver electrodes were attached on both sides, and then, the resistance of the sample was measured. On the basis of the resistance, the electrical conductivity can be calculated with the following equation as follows:

$$\sigma = 1/\rho = d/RS \quad (1)$$

where σ is the electrical conductivity, ρ is the resistivity, R is the resistance, d is the sample thickness, and S is the cross-sectional area of the sample. Three to four replicate samples were prepared and measured with different AgNW contents.

3. RESULTS AND DISCUSSION

The synthesized PS microspheres were characterized by SEM. Figure 2 shows a photomicrograph of the PS microspheres prepared by the emulsifier-free emulsion polymerization. The average diameter of the PS microspheres was ca. 500 nm with well-ordered monodisperse spherical pattern. The number-average and weight-average molecular weights by gel permeation chromatography were 45 000 g/mol and 229 000 g/mol, respectively, which have relatively high polydispersity in molecular weight. A polyol process has been successfully used for the synthesis of AgNWs, in which a PVP stabilizer is used as a capping agent to induce the direct growth of 1D nanowires.[21] The surface morphology of AgNWs depends on the concentrations of the starting materials, reaction time, and temperature.[18,19] The synthesized AgNWs were characterized by FE-SEM, and the corresponding micrograph of the AgNWs is shown in Figure 3. The length and diameter of the nanowires can be measured from images such as the one shown in Figure S1b in the Supporting Information. These data are shown in

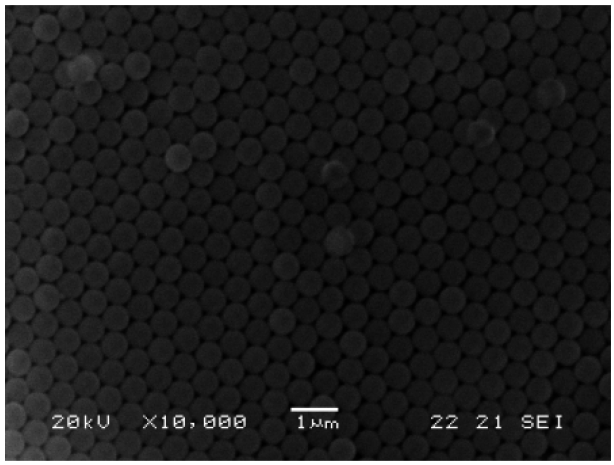

Figure 2. SEM image of the PS microspheres prepared by emulsifier-free emulsion polymerization.

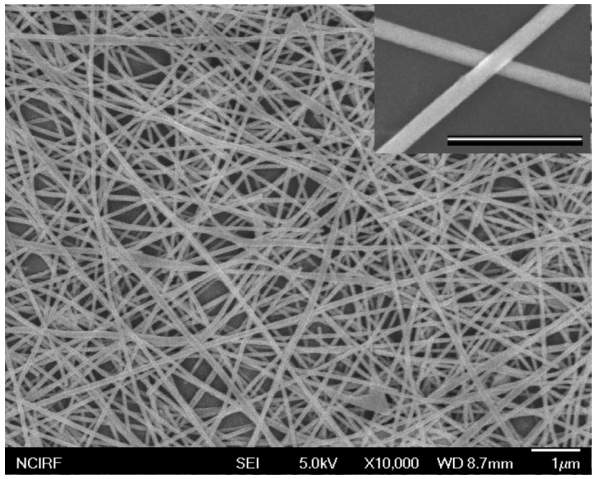

Figure 3. FE-SEM image of purified AgNWs synthesized by the polyol process. (inset) A magnified image estimating the AgNW diameter (scale bar of 1 μm).

Figure S2 in the Supporting Information in the form of histograms of the length and diameter, respectively. It reveals that the length varied from 10 to 60 μm with a mean of 35 ± 7 μm, and the diameter varied from 70 to 140 nm with a mean of 112 ± 13 nm. The crystalline nature of the AgNWs was also identified by XRD and XPS techniques. Figure S3 in the Supporting Information shows the XRD patterns of the AgNWs synthesized by the polyol process. The four major peaks corresponded to the (111), (200), (220), and (311) crystallographic planes of silver crystal (JCPDS card No. 04–0783), which indicate that the AgNWs had a pure crystalline nature and can be indexed as face-centered cubic (FCC) silver.[28] The absence of other peaks corresponding to any impurities or organic moieties confirms the quality of the prepared AgNWs.[29] XPS also verified the purity and chemical state of the synthesized AgNWs. Figure S4 in the Supporting Information shows the XPS wide scan spectrum and the Ag 3d and O 1s deconvoluted spectra of the AgNWs. The deconvoluted spectrum with two peaks at ~367.7 and 373.8 eV corresponding to Ag $3d_{5/2}$ and Ag $3d_{3/2}$ respectively, confirms the presence of metallic silver. Existence of strong chemical interaction between PVP and AgNWs is confirmed by XPS spectrum in the region of O 1s. In the case of PVP-capped

DOI: 10.1021/am5071392
ACS Appl. Mater. Interfaces 2015, 7, 756–764

AgNWs, the peak attributed to O 1s (532.0 eV) is shifted toward higher binding energy compared with pure PVP (530.3 eV).[30] The positively shifted O 1s binding energy originates from the weakness of electron density around O atoms in the carbonyl group of PVP, implying that the surfaces of AgNWs strongly coordinate with O atoms in PVP.[30] Thus, the coordination interaction of PVP on the surface of AgNWs restricts the radial growth of the AgNWs. Taking the consistent outcomes of FE-SEM, XRD and XPS altogether, it is concluded that AgNWs were successfully synthesized, and they were present in metallic form encapsulated by PVP molecules around them.

The UV−vis spectroscopic method can also be used to track the morphological evolution involved in the growth process because silver nanomaterials with different shapes exhibit different surface plasmon resonance (SPR) bands.[31] Figure 4

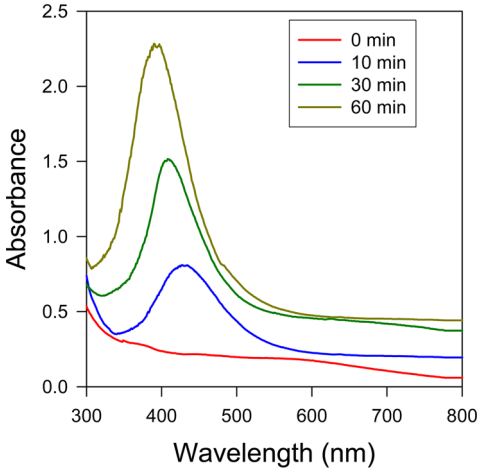

Figure 4. UV−vis spectra showing the formation of AgNWs with reaction time.

shows the UV−vis spectra of the AgNWs at different stages of the polyol process. As the reaction proceeded, the intensity of the plasmon band almost tripled, and the peak became narrower, which indicates an increase in the number of nanomaterials in the reaction solution and the uniformity of the nanomaterials through Ostwald ripening.[16] The rapid enhancement of the peak intensity at 400 nm implies that the number of Ag nanorods grew quickly into nanowires.[32] As the reaction continued, the transverse SPR band positioned at ∼420 nm slightly shifted to the blue side at ∼390 nm, indicating the formation of high aspect ratio AgNWs.[30]

Figure 5 shows the dispersion and distribution of the AgNWs in the PS/AgNW nanocomposite powder prepared with latex blending. It seems that the AgNWs are randomly distributed and clearly display the dispersion of individual nanowire over the entire region of PS microspheres in which the presence of high aspect ratio AgNWs is evident. When the silver concentration was increased to 3 vol %, a higher density of AgNWs in the nanocomposite powder was also observed. Furthermore, it appears that the AgNWs formed numerous networks with random contacts between neighboring AgNWs. Aggregation or bundles of AgNWs were practically absent from the nanocomposite powder, even for the powder with a higher AgNW concentration (3 vol %). Once molded, AgNWs are likely to be distributed forming an AgNW network structure throughout the polymer matrix while maintaining a high degree

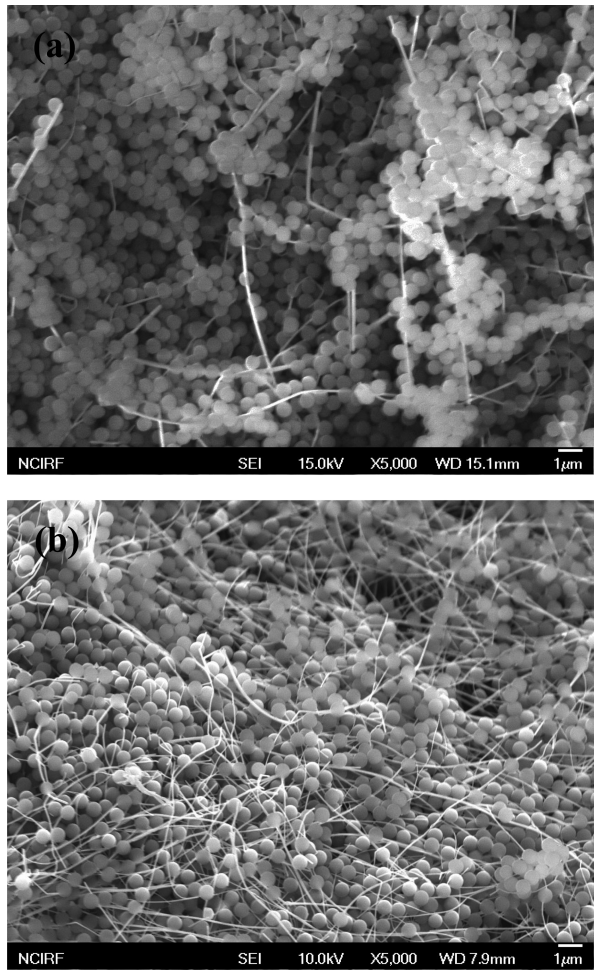

Figure 5. FE-SEM images of freeze-dried PS/AgNW nanocomposite powder showing the extent of AgNW dispersion: (a) 1 vol % AgNWs and (b) 3 vol % AgNWs.

of homogeneous dispersion in the polymer.[33] Conductive nanowires do not develop electrostatic affinities and prevent them from agglomeration. This will help approve some interaction between PS matrix and PVP-capped AgNWs. To confirm the purity of the AgNWs, EDS was also analyzed, and the results are presented in Table S1 and Figure S5 in the Supporting Information. The EDS results show that there are C and Ag elements in the sample. The Ag comes from the AgNWs, and the C moiety originates from the polymer matrix. Moreover, the EDS results clearly show the absence of oxides and other inorganic moieties indicating the purity of the AgNWs in the polymer nanocomposites. This analysis also confirmed the amount of AgNWs present in the PS/AgNW nanocomposites.[34]

Cross-sectional views of the molded nanocomposite samples were examined to assess the distribution of nanofillers across the sample thickness. Molded specimens of PS/AgNW nanocomposite powder were fractured after immersion and rapid freezing in liquid nitrogen. Figure 6 shows the fractured surfaces of the PS polymer matrix incorporated with 1 vol % of AgNWs compared to the sample prepared by coagulated precipitation. The fracture image of the sample prepared by latex blending shows good dispersion of the AgNWs in the PS matrix, comparing the image of the coagulated precipitation sample. In Figure 6a, the randomly oriented nanofiber-like

DOI: 10.1021/am5071392
ACS Appl. Mater. Interfaces 2015, 7, 756−764

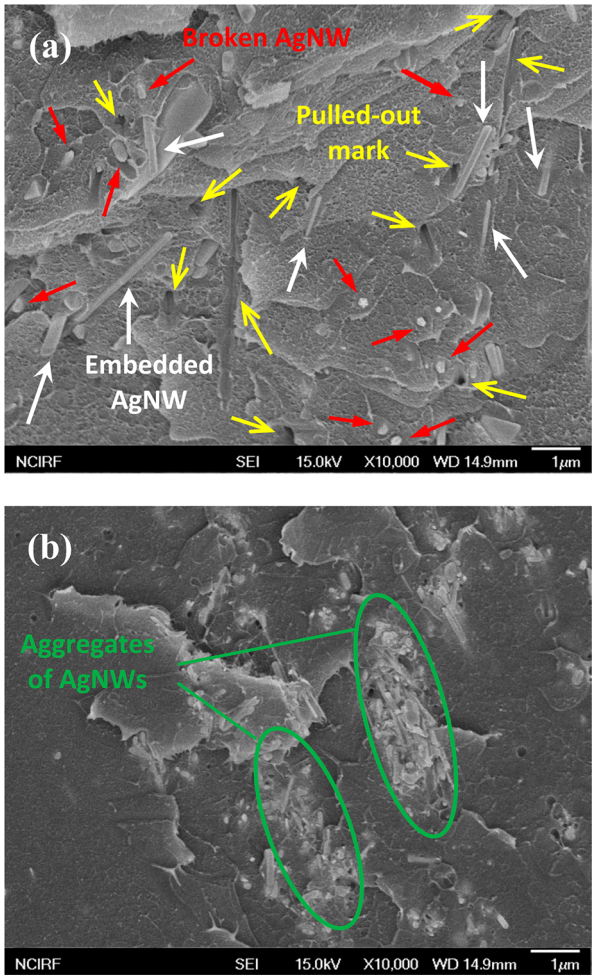

Figure 6. FE-SEM images of the fracture surface of the PS/AgNW (1 vol %) nanocomposite samples: (a) prepared by latex blending and (b) prepared by coagulated precipitation.

domains penetrating throughout the PS matrix show that the AgNWs are well-dispersed in the PS matrix.[33] Independently existing pulled-out marks and embedded and broken AgNWs by latex blending indicate high degree of dispersion of AgNWs without agglomeration. Individual AgNWs are observed in all orientations and appear to form a network with random contacts between adjacent AgNWs. The random network structure connected by the high aspect ratio nanofillers is a prospective candidate for conductive device development. Because the AgNWs synthesized by the polyol method are encapsulated by hydrophilic PVP, it seems much easier to disperse the AgNWs in an aqueous suspension containing PS microspheres than in a hydrophobic solution of PS dissolved in toluene, resulting in AgNW agglomerates seen in Figure 6b. In addition, attractive interactions between PS microspheres and PVP-capped AgNWs also contribute to generate agglomeration-free polymer nanocomposites. Elemental mapping of fracture surface of the nanocomposite also clearly showed good distribution of AgNWs across the sample cross section (image not shown in this study). All these results suggest that the latex blending methodology provides suitable conductive polymer nanocomposites.

The load of AgNWs in the prepared nanocomposites was determined by TGA, which was also used to analyze the thermal degradation of the nanocomposites. The TGA curve in Figure 7 shows the characteristic degradation process of the PS/AgNW nanocomposites. Because silver is thermally stable

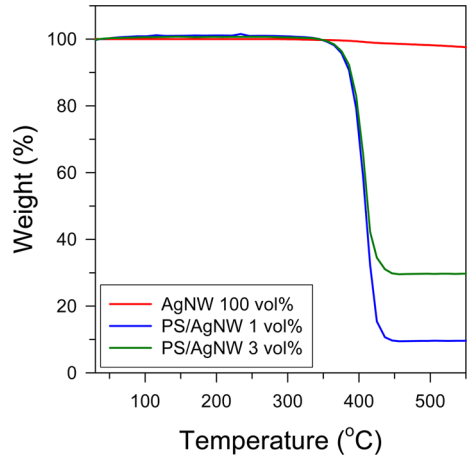

Figure 7. Thermogravimetric analysis curves of the PS/AgNW nanocomposites.

at 600 °C, it is certain that the marginal mass loss found in the AgNW 100 vol % is caused by the degradation of the PVP encapsulating the AgNWs.[35] In the PS/AgNW nanocomposites, the main step of mass loss begins at ∼365 °C and continues until the temperature reaches 430 °C. The char yields of the nanocomposites with AgNW contents of 1 and 3 vol % confirmed the amount of AgNWs in the polymer matrix. As expected, the weight remaining proportionally increased with the increase of AgNW content. However, increasing the AgNW content slightly increased the thermal stability of the nanocomposites, showing almost similar degrading pattern compared to that of the lower content.

The viscoelastic properties of the polymer/nanofiller composites have scientific importance probing the composite dynamics and microstructure.[6] In the same manner, the rheological properties of the PS/AgNW nanocomposites can be used to predict the degree of the AgNW dispersion in the PS matrix. The storage modulus G', loss modulus G'', and complex viscosity η^* of the PS/AgNW nanocomposites with respect to the AgNW content are shown in Figure 8. By increasing the angular frequency, the storage and loss moduli increased, and the complex viscosity decreased. The storage and loss moduli and the complex viscosity strongly increased with a small addition of AgNW 1 vol % at low frequencies, and their increments became weaker with increasing frequency due to shear thinning; in other words, the effect of AgNW addition was much higher at lower frequencies than at higher frequencies. Even in the case of AgNW 1 vol % addition, a networklike structure seems to be formed due to randomly oriented contacts between nanowires, and as a result, the storage modulus at low frequencies showed a dramatic increase, and the slope became less steep indicating a change from a liquid-like response to a solid-like response. It can be also found that the corresponding increase in the loss modulus is much lower than the storage modulus, which represents increased solid-like behavior with the increase of AgNWs. The complex viscosity showed the typical flow behavior of shear thinning polymer melts, revealing a Newtonian plateau at low frequencies and shear thinning at high frequencies. At low frequencies, the rheological behavior exhibited a solid-like response representing the characteristics similar to yield stress

DOI: 10.1021/am5071392
ACS Appl. Mater. Interfaces 2015, 7, 756−764

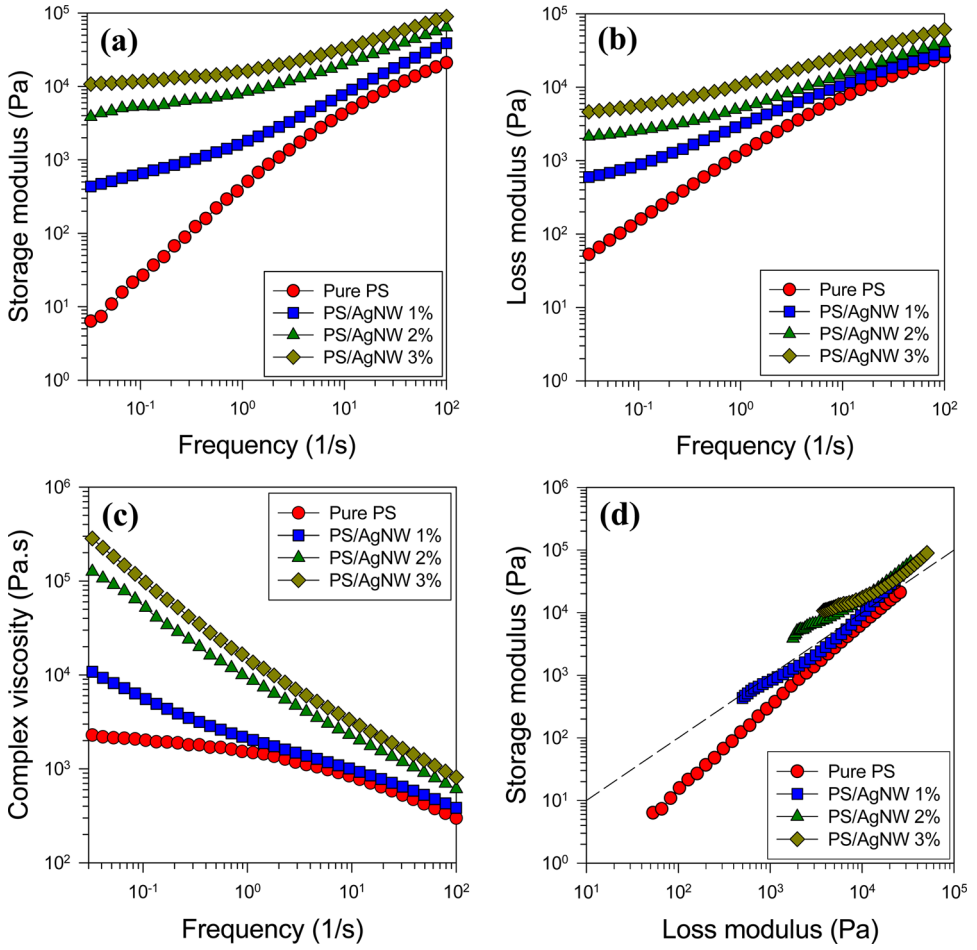

Figure 8. Effect of AgNW content on the rheological properties of the PS/AgNW nanocomposites (strain amplitude: 3%): (a) storage modulus, (b) loss modulus, (b) complex viscosity, and (d) storage modulus vs loss modulus.

behavior. It has amply been demonstrated that the existence of a yield stress is associated with polymer and nanofiller interactions and with the formation of a nanoscale network of polymer chains and nanofillers.[36] In contrast, the rheological properties at high frequencies will mainly be determined by the polymer matrix because the attraction between nanowires gets weaker due to the high shear action and the alignment of rodlike fillers to flow direction leads to lower viscosities. Thus, the characteristic rheological response can be used to monitor the degree of nanofiller dispersion and the extent of nanostructure formation.

In multiphase polymer systems, the plots of the storage modulus versus the loss modulus analogous to Cole−Cole plots can be applied to map out structural differences between the matrix and filled system at a given temperature.[37] Figure 8d shows the log G' versus log G'' plots for the PS/AgNW nanocomposites. The short dash line represents a guidance line that shows G' and G'' are equal. A plot passing through this line from below is considered to represent rheological behavior changing from viscous to elastic. If a plot lies above this line (i.e., G' is always greater than G''), this indicates that the nanocomposite shows elasticity-dominant behavior over the whole frequency region. As shown in Figure 8d, the storage modulus increased with increasing AgNW content for a given loss modulus. With increasing AgNW content, the slope of the log G' versus log G'' plots was decreased. The slope change and shift in the log G' versus log G'' plots indicate that the microstructure of the PS/AgNW nanocomposites changed significantly with the addition of AgNWs. Moreover, with the addition of 2 vol % and 3 vol % AgNWs, the curves of log G' versus log G'' nearly coincide, revealing that the microstructure did not change much with further addition of AgNWs. Above the addition of 2 vol % AgNWs, the storage modulus appears to lie above the loss modulus across all frequencies. Lastly, the rheological properties of the corresponding nanocomposites prepared by coagulated precipitation were presented for comparison in Figure S6 in the Supporting Information. The comparison of two cases indicates that the AgNWs are dispersed better in the PS matrix in the case of latex-blending method compared to the case of coagulated precipitation method.

The electrical conductivity of polymer nanocomposites is affected by the content, dispersion and distribution,[38] aspect ratio,[39] and alignment[40] of conducting nanofillers. Figure 9 shows the effect of the AgNW content on the electrical conductivity, comparing the two cases prepared by latex blending and coagulated precipitation. The electrical properties of the PS/AgNW nanocomposites depended sharply on the AgNW content showing typical percolation behavior. The nanocomposites did not show electrical conductivity similar to that of pure PS below a certain concentration level and showed a sharp increase in electrical conductivity indicating the formation of conductive networks above a critical concentration, that is, the percolation threshold. It can be expected

DOI: 10.1021/am5071392
ACS Appl. Mater. Interfaces 2015, 7, 756−764

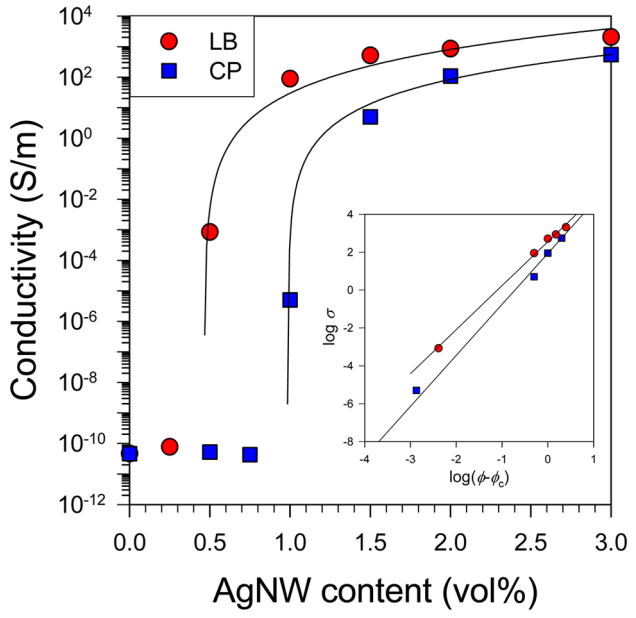

Figure 9. Effect of AgNW content on the electrical conductivity of the PS/AgNW nanocomposites, for which the two methods prepared by latex blending (LB) and coagulated precipitation (CP) were compared. (inset) The linear fitting of the data to the power law equation for electrical conductivity. The percolation threshold ϕ_c of LB and CP is 0.489 vol % and 0.988 vol %, and the critical exponent b of LB and CP is 2.13 and 2.69, respectively.

that geometrical connectivity formed above the percolation threshold leads to a dramatic increase in electrical conductivity. However, there exists another possibility that cannot be ruled out since potential barriers such as gap, surfactant, or monolayer coating can be formed in many systems, such as various composites.[41−44] In this case, the electrical conductivity can be attributed to quantum mechanical tunneling and hopping of electrons within a critical separation distance.[41,44] Nevertheless, it is generally accepted that polymer composites and nanocomposites conform well to the percolation threshold theory. The percolation threshold is typically determined by plotting the electrical conductivity as a function of the nanofiller content and fitting with a power law relationship as follows:

$$\sigma \propto (\phi - \phi_c)^b \quad (2)$$

where ϕ is the volume percent of the nanofiller; ϕ_c is the electrical percolation threshold for the vol %, and b is the critical exponent relating to the system dimension. Percolation threshold values of 0.489 and 0.988 vol % were obtained for the samples prepared by latex blending and coagulated precipitation, respectively. The inset in Figure 9 shows the best regression fits using the power law relationship. The PS/AgNW nanocomposite prepared by latex blending showed much lower percolation threshold compared to that by coagulated precipitation, indicating that the former forms a more effective network structure with good dispersion of the AgNWs in the matrix PS than the latter. Fracture surface images of the nanocomposites shown in Figure 6 also confirm that the electrical conductivity between AgNWs is closely dependent on the morphology of the nanocomposites. Moreover, the critical exponent b in the power law relationship is a barometer related to the microstructural properties of composites.[45] It is reported that calculated values of the critical exponent are between 1.6 to 2.0, and experimental values are in the range of 1.5 to 2.0 for 3D network systems of conductive spherical particles in an insulating matrix.[46] For systems filled with 1D fiber-filled systems as in this study, b values higher than 2 have been known.[8,46] The values of 2.13 and 2.69 produced in this work are in good agreement with the data in the literature. The electrical conductivity prepared by latex blending reached higher than 10^2 and 10^3 S/m with the addition of 1 and 3 vol % of AgNWs, respectively. The electrical conductivity of the PS/AgNW nanocomposites is several orders of magnitude higher than that of the PS/CNT nanocomposites.[26,47−49] It is speculated that the enhanced electrical properties for the PS/AgNW nanocomposites are possible because of the highly crystalline structure of the AgNWs with high aspect ratio synthesized by the polyol method and the excellent degree of AgNW dispersion prepared by the latex-blending process.

4. CONCLUSIONS

Electrically conductive polymer nanocomposites incorporated with metallic nanowires can be prepared with the latex-blending process, which utilizes freeze-drying an aqueous suspension system comprised of polymer microspheres and nanofillers. This technology does not require surfactant or surface modifications by chemical or physical treatments to endow good affinity and dispersion between the polymer and nanofillers during mixing and results in highly conductive nanocomposites. In this study, polystyrene and silver were chosen as the matrix polymer and metallic nanofiller. Highly monodisperse PS microspheres were synthesized by emulsifier-free emulsion polymerization, and high aspect ratio AgNWs were synthesized with the polyol method. The PS/AgNW nanocomposites exhibited a well-dispersed morphology and enhanced electrical conductivity. The rheological properties of the nanocomposites confirm that the material state changes from liquid-like to solid-like as the AgNW content increases, indicating a physical network formation of AgNWs. The PS/AgNW nanocomposites prepared by latex blending had an electrical percolation threshold of 0.49 vol % AgNWs and electrical conductivities higher than 10^2 S/m and 10^3 S/m at 1 and 3 vol % AgNWs, respectively. It is expected that the electrically conductive polymer nanocomposites with well-dispersed AgNWs will be a promising material for the development of EMI shielding materials, flexible optoelectronic devices, sensors, and actuators in the near future.

■ ASSOCIATED CONTENT

Supporting Information

SEM images and size-distribution graph, XRD patterns and XPS spectra of AgNWs, EDS spectra of PS/AgNW nanocomposites, and rheological properties of PS/AgNW nanocomposites prepared by coagulated precipitation. This material is available free of charge via the Internet at http://pubs.acs.org.

■ AUTHOR INFORMATION

Corresponding Author

*Phone: +82-31-220-2235. Fax: +82-31-220-2494. E-mail: sjlee@suwon.ac.kr.

Notes

The authors declare no competing financial interest.

DOI: 10.1021/am5071392
ACS Appl. Mater. Interfaces 2015, 7, 756−764

■ ACKNOWLEDGMENTS

The authors gratefully acknowledge the National Research Foundation of Korea (NRF) under the Ministry of Education, Science, and Technology (MEST) for the financial support (Grant Nos. 2011-0011180 and 2013R1A2A2A07067387).

■ REFERENCES

(1) Balazs, A. C.; Emrick, T.; Russell, T. P. Nanoparticle Polymer Composites: Where Two Small Worlds Meet. *Science* **2006**, *314*, 1107−1110.
(2) Gangopadhyay, R.; De, A. Conducting Polymer Nanocomposites: a Brief Overview. *Chem. Mater.* **2000**, *12*, 608−622.
(3) Lu, X.; Zhang, W.; Wang, C.; Wen, T. C.; Wei, Y. One-Dimensional Conducting Polymer Nanocomposites: Synthesis, Properties and Applications. *Prog. Polym. Sci.* **2011**, *36*, 671−712.
(4) Murphy, C. J.; Jana, N. R. Controlling the Aspect Ratio of Inorganic Nanorods and Nanowires. *Adv. Mater.* **2002**, *14*, 80−82.
(5) Sandler, J. K. W.; Kirk, J. E.; Kinloch, I. A.; Shaffer, M. S. P.; Windle, A. H. Ultra-Low Electrical Percolation Threshold in Carbon-Nanotube-Epoxy Composites. *Polymer* **2003**, *44*, 5893−5899.
(6) Moniruzzaman, M.; Winey, K. I. Polymer Nanocomposites Containing Carbon Nanotubes. *Macromolecules* **2006**, *39*, 5194−5205.
(7) Byrne, M. T.; Gun'ko, Y. K. Recent Advances in Research on Carbon Nnaotube-Polymer Composites. *Adv. Mater.* **2010**, *22*, 1672−1688.
(8) Gelves, G. A.; Al-Saleh, M. H.; Sundararaj, U. Highly Electrically Conductive and High Performance EMI Shielding Nanowire/Polymer Nanocomposites by Miscible Mixing and Precipitation. *J. Mater. Chem.* **2011**, *21*, 829−836.
(9) Tjong, S. C. Structural and Mechanical Properties of Polymer Nanocomposites. *Mater. Sci. Eng. R* **2006**, *53*, 73−197.
(10) Gelves, G. A.; Lin, B.; Sundararaj, U.; Haber, J. A. Low Electrical Percolation Threshold of Silver and Copper Nanowires in Polystyrene Composites. *Adv. Funct. Mater.* **2006**, *16*, 2423−2430.
(11) Lee, J.; Lee, P.; Lee, H.; Lee, D.; Lee, S. S.; Ko, S. H. Very Long Ag Nanowire Synthesis and Its Application in a Highly Transparent, Conductive and Flexible Metal Electrode Touch Panel. *Nanoscale* **2012**, *4*, 6408−6414.
(12) Maiti, S.; Shrivastava, N. K.; Suin, S.; Khatua, B. B. Polystyrene/MWCNT/Graphite Nanoplate Nanocomposites: Efficient Electromagnetic Interference Shielding Material through Graphite Nanoplate−MWCNT−Graphite Nanoplate Networking. *ACS Appl. Mater. Interfaces* **2013**, *5*, 4712−4724.
(13) Hu, M.; Gao, J.; Dong, Y.; Li, K.; Shan, G.; Yang, S.; Li, R. K. Y. Flexible Transparent PES/Silver Nanowires/PET Sandwich-Structured Film for High-efficiency Electromagnetic Interference Shielding. *Langmuir* **2012**, *28*, 7101−7106.
(14) Xu, J.; Munari, A.; Dalton, E.; Mathewson, A.; Razeeb, K. M. Silver Nanowire Array-Polymer Composite as Thermal Interface Material. *J. Appl. Phys.* **2009**, *106*, 124310.
(15) Zeng, X. Y.; Zhang, Q. K.; Yu, R. M.; Lu, C. Z. A New Transparent Conductor: Silver Nanowire Film Buried at the Surface of a Transparent Polymer. *Adv. Mater.* **2010**, *22*, 4484−4488.
(16) Chen, D.; Qiao, X.; Qiu, X.; Chen, J.; Jiang, R. Convenient Synthesis of Silver Nanowires with Adjustable Diameters via a Solvothermal Method. *J. Colloid Interface Sci.* **2010**, *344*, 286−291.
(17) Mazur, M. Electrochemically Prepared Silver Nanoflakes and Nanowires. *Electrochem. Commun.* **2004**, *6*, 400−403.
(18) Korte, K. E.; Skrabalak, S. E.; Xia, Y. Rapid Synthesis of Silver Nanowires through a CuCl- or $CuCl_2$-Mediated Polyol Process. *J. Mater. Chem.* **2008**, *18*, 437−441.
(19) Sun, Y.; Mayers, B.; Herricks, T.; Xia, Y. Polyol Synthesis of Uniform Silver Nanowires: a Plausible Growth Mechanism and the Supporting Evidence. *Nano Lett.* **2003**, *3*, 955−960.
(20) Sun, Y.; Xia, Y. Large-Scale Synthesis of Uniform Silver Nanowires Through a Soft, Self-Seeding, Polyol Process. *Adv. Mater.* **2002**, *14*, 833−837.
(21) Wiley, B.; Sun, Y.; Mayers, B.; Xia, Y. Shape-Controlled Synthesis of Metal Nanostructures: The Case of Silver. *Chem.—Eur. J.* **2005**, *11*, 454−463.
(22) Tsuji, M.; Nishizawa, Y.; Hashimoto, M.; Tsuji, T. Syntheses of Silver Nanofilms, Nanorods, and Nanowires by a Microwave-Polyol Method in the Presence of Pt Seeds and Polyvinylpyrrolidone. *Chem. Lett.* **2004**, *33*, 370−371.
(23) Bai, J. B.; Allaoui, A. Effect of the Length and the Aggregate Size of MWNTs on the Improvement Efficiency of the Mechanical and Electrical Properties of Nanocomposites—Experimental Investigation. *Composites, Part A* **2003**, *34*, 689−694.
(24) Liu, Q.; Tu, J.; Wang, X.; Yu, W.; Zheng, W.; Zhao, Z. Electrical Conductivity of Carbon Nanotube/Poly(vinylidene fluoride) Composites Prepared by High-Speed Mechanical Mixing. *Carbon* **2012**, *50*, 339−341.
(25) Ramanathan, T.; Abdala, A. A.; Stankovich, S.; Dikin, D.; Herrera-Alonso, M.; Piner, R. D.; Adamson, D. H.; Schniepp, H. C.; Chen, X.; Ruoff, R. S.; Nguyen, S. T.; Aksay, I. A.; Prud'Homme, R. K.; Brinson, L. C. Functionalized Graphene Sheets for Polymer Nanocomposites. *Nat. Nanotechnol.* **2008**, *3*, 327−331.
(26) Wu, T. M.; Chen, E. C. Preparation and Characterization of Conductive Carbon Nanotube−Polystyrene Nanocomposites Using Latex Technology. *Compos. Sci. Technol.* **2008**, *68*, 2254−2259.
(27) Woo, D. K.; Kim, B. C.; Lee, S. J. Preparation and Rheological Behavior of Polystyrene/Multi-Walled Carbon Nanotube Composites by Latex Technology. *Korea-Aust. Rheol. J.* **2009**, *21*, 185−191.
(28) Sun, X.; Li, Y. Cylindrical Silver Nanowires: Preparation, Structure, and Optical Properties. *Adv. Mater.* **2005**, *17*, 2626−2630.
(29) Chen, C.; Wang, L.; Jiang, G.; Zhou, J.; Chen, X.; Yu, H.; Yang, Q. Study on the Synthesis of Silver Nanowires with Adjustable Diameters through the Polyol Process. *Nanotechnology* **2006**, *17*, 3933−3938.
(30) Gao, Y.; Jiang, P.; Song, L.; Liu, L.; Yan, X.; Zhou, Z.; Liu, D.; Wang, J.; Yuan, H.; Zhang, Z.; Zhao, X.; Dou, X.; Zhou, W.; Wang, G.; Xie, S. Growth Mechanism of Silver Nanowires Synthesized by Polyvinylpyrrolidone-Assisted Polyol Reduction. *J. Phys. D: Appl. Phys.* **2005**, *38*, 1061−1067.
(31) Song, M. X.; Feng, J. Y.; Li, W.; Hu, Q.; Zhang, Z. Z.; Liu, B. F.; Zhao, X. J. Synthesis and Characterization of Silver Nanowires by Solvothermal. *Adv. Mater. Res.* **2009**, *66*, 159−162.
(32) Zhu, J. J.; Kan, C. X.; Wan, J. G.; Han, M.; Wang, G. H. High-Yield Synthesis of Uniform Ag Nanowires with High Aspect Ratios by Introducing the Long-Chain PVP in an Improved Polyol Process. *J. Nanomater.* **2011**, *2011*, 982547.
(33) Mi, H. Y.; Li, Z.; Turng, L. S.; Sun, Y.; Gong, S. Silver Nanowire/Thermoplastic Polyurethane Elastomer Nanocomposites: Thermal, Mechanical, and Dielectric Properties. *Mater. Des.* **2014**, *56*, 398−404.
(34) Zong, R. L.; Zhou, J.; Li, Q.; Du, B.; Li, B.; Fu, M.; Qi, X. W.; Li, L. T.; Buddhudu, S. Synthesis and Optical Properties of Silver Nanowire Arrays Embedded in Anodic Alumina Membrane. *J. Phys. Chem. B* **2004**, *108*, 16713−16716.
(35) Tamboli, M. S.; Kulkarni, M. V.; Patil, R. H.; Gade, W. N.; Navale, S. C.; Kale, B. B. Nanowires of Silver−Polyaniline Nanocomposite Synthesized via in Situ Polymerization and Its Novel Functionality as an Antibacterial Agent. *Colloids Surf., B* **2012**, *92*, 35−41.
(36) Lin, B.; Gelves, G. A.; Haber, J. A.; Sundararaj, U. Electrical, Rheological, and Mechanical Properties of Polystyrene/Copper Nanowire Nanocomposites. *Ind. Eng. Chem. Res.* **2007**, *46*, 2481−2487.
(37) Lee, K. M.; Han, C. D. Rheology of Organoclay Nanocomposites: Effects of Polymer Matrix/Organoclay Compatibility and the Gallery Distance of Organoclay. *Macromolecules* **2003**, *36*, 7165−7178.
(38) Al-Saleh, M. H.; Sundararaj, U. A Review of Vapor Grown Carbon Nanofiller/Polymer Conductive Composites. *Carbon* **2009**, *47*, 2−22.

DOI: 10.1021/am5071392
ACS Appl. Mater. Interfaces 2015, 7, 756−764

(39) Bryning, M. B.; Islam, M. F.; Kikkawa, J. M.; Yodh, A. G. Highly Electrically Conductive and High Performance EMI Shielding Nanowire/Polymer Nanocomposites by Miscible Mixing and Precipitation. *Adv. Mater.* **2005**, *17*, 1186−1191.
(40) Du, F.; Scogna, R. C.; Zhou, W.; Brand, S.; Fischer, J. E.; Winey, K. I. Nanotube Networks in Polymer Nanocomposites: Rheology and Electrical Conductivity. *Macromolecules* **2004**, *37*, 9048−9055.
(41) Balberg, I. Tunnelling and Percolation in Lattices and the Continuum. *J. Phys. D: Appl. Phys.* **2009**, *42*, 064003.
(42) Ambrosetti, G.; Grimaldi, C.; Balberg, I.; Maeder, T.; Danani, A.; Ryser, P. Solution of the tunneling-Percolation Problems in the Nanocomposite Regime. *Phys. Rev. B: Condens. Matter Mater. Phys.* **2010**, *81*, 155434.
(43) Wu, H.; Liu, J.; Wu, X.; Ge, M.; Wang, Y.; Zhang, G.; Jiang, J. High Conductivity of Isotropic Conductive Adhesives Filled with Silver Nanowires. *Int. J. Adhes. Adhes.* **2006**, *26*, 617−621.
(44) Balberg, I.; Azulay, D.; Toker, D.; Millo, O. Percolation and Tunneling in Composite Materials. *Int. J. Mod. Phys. B* **2004**, *18*, 2091−2121.
(45) Hu, G.; Zhao, C.; Zhang, S.; Yang, M.; Wang, Z. Low Percolation Thresholds of Electrical Conductivity and Rheology in Poly(ethylene terephthalate) through the Networks of Multi-Walled Carbon Nanotubes. *Polymer* **2006**, *47*, 480−488.
(46) Weber, M.; Kamal, M. R. Estimation of the Volume Resistivity of Electrically Conductive Composites. *Polym. Compos.* **1997**, *18*, 711−725.
(47) Yu, J.; Lu, K.; Sourty, E.; Grossiord, N.; Koning, C. E.; Loos, J. Characterization of Conductive Multiwall Carbon Nanotube/Polystyrene Composites Prepared by Latex Technology. *Carbon* **2007**, *45*, 2897−2903.
(48) Kota, A. K.; Cipriano, B. H.; Duesterberg, M. K.; Gershon, A. L.; Powell, D.; Raghavan, S. R.; Bruck, H. A. Electrical and Rheological Percolation in Polystyrene/MWCNT Nanocomposites. *Macromolecules* **2007**, *40*, 7400−7406.
(49) Kara, S.; Arda, E.; Dolastir, F.; Pekcan, Ö. Electrical and Optical Percolations of Polystyrene Latex−Multiwalled Carbon Nanotube Composites. *J. Colloid Interface Sci.* **2010**, *344*, 395−401.

DOI: 10.1021/am5071392
ACS Appl. Mater. Interfaces 2015, 7, 756−764